Overview of Results in the MST Reversed-Field Pinch Experiment

J.S. Sarff 1), G.F. Abdrashitov 2), A. Alfier 3), A.F. Almagri 1), J.K. Anderson 1), F. Auriemma 3), W.F. Bergerson 4), F. Bonomo 3), M.T. Borchardt 1), D.L. Brower 4), D.R. Burke 1), K. Caspary 1), B.E. Chapman 1), D.J. Clayton 1), S. Combs 5), D. Craig 6), H.D. Stephens 1), V.I. Davydenko 2), P.P. Deichuli 2), D.R. Demers 7), D.J. Den Hartog 1), W.X. Ding 4), F. Ebrahimi 1), A. Falkowski 1), A. Fassina 3), G. Fiksel 8), P. Fimognari 1), C. Foust 5), C.B. Forest 1), P. Franz 3), J.A. Goetz 1), M. Gobbin 3), W. Harris 1), R.W. Harvey 1), D.J. Holly 1), A.A. Ivanov 2), M.C. Kaufman 1), J. Ko 1), J. Koliner 1), V. Kolmogorov 2), S. Kumar 1), J.D. Lee 1), L. Lin 4), D. Liu 1), R. Lorenzini 3), R.M. Magee 1), K.J. McCollam 1), M. McGarry 1), M.C. Miller 1), V.V. Mirnov 1), M.D. Nornberg 1), P.D. Nonn 1), S.P. Oliva 1), E. Parke 1), P. Piovesan 3), J.A. Reusch 1), A. Seltzman 1), D. Spong 5), D. Stone 1), N.V. Stupishin 2), D. Theucks 1), V. Tangri 1), P.W. Terry 1), T.D. Tharp 1), J. Waksman 1), Y.M. Yang 1), T.F. Yates 4), P. Zanca 3)

1) University of Wisconsin, Madison, Wisconsin, and the Center for Magnetic Self-
   Organization in Laboratory and Astrophysical Plasmas
2) Budker Institute of Nuclear Physics, Novosibirsk, Russia
3) Consorzio RFX, Associazione EURATOM-ENEA sulla Fusione, Padova, Italy
4) The University of California at Los Angeles, Los Angeles, California
5) The Oak Ridge National Laboratory, Oak Ridge, Tennessee
6) Wheaton College, Wheaton, Illinois
7) Rensselaer Polytechnic Institute, Troy, New York
8) Laboratory for Laser Energetics, University of Rochester, New York

E-mail contact of main author: jssarff@wisc.edu

Abstract: An overview of MST results is presented. Substantial advances have been achieved in RFP confinement, in the development of auxiliary sources for heating and current drive, and in studies of fluctuations, transport, and magnetic self-organization physics. The density in improved confinement plasmas has been increased above the empirical limit, n/n_G=1.5, using pellet injection. A record density of 0.7×10^{20} m^{-3} has been achieved in high current (0.5 MA) plasmas. Maximum energy confinement is attained at 0.5 MA and lower n/n_G=0.13; this establishes confinement comparable to a same-size, same-current tokamak over MST's full range of plasma current. Experiments using a new 1 MW, 25 keV neutral beam injector are underway, to explore beta limits, energetic particle confinement, momentum transport, and current profile control. Analysis of the d-d neutron production evidences good fast ion confinement. Results for oscillating field current drive are in good agreement with nonlinear resistive MHD computation, bolstering the OFCD physics basis. Energy confinement with OFCD is measured comparable to that for standard induction. Non-collisional ion heating generates transient temperatures T_i=2-3 keV. The heating efficiency is measured to scale with a fractional power of the ion mass, and to be anisotropic depending on the plasma density. Broadband magnetic turbulence exhibits a dissipative nonlinear cascade that could be connected to the ion heating mechanism. A new high rep-rate Thomson scattering diagnostic measures electron temperature fluctuations associated with residual magnetic islands and helical mode structure. The equilibrium and fluctuations of quasi-single-helicity plasmas are investigated with this and MST's other advanced diagnostics. Lower hybrid and electron Bernstein wave injection (~100 kW absorbed power for each) are in development for current drive and heating.

1. Introduction

This overview of results from the MST reversed-field pinch (RFP) reports substantial advances achieved in RFP confinement, in the development of auxiliary sources for heating and current drive, and in studies of fluctuations, transport, and magnetic self-organization. The MST is a large RFP device (R =1.5 m, a =0.5 m) that operates at medium plasma current

($I_p \leq 0.55$ MA). The RFP magnetic configuration offers several potential advantages for fusion as a result of the concentration of magnetic field within the plasma, including the possibility for normal magnets, a high particle density limit commensurate with high plasma current density operation, and the possibility for Ohmic heating to burning plasma conditions. These features promote a reactor vision for high power density and high reliability through the use of relatively simple technology. The RFP's large magnetic shear and weaker toroidal effects provide valuable physics contrast to tokamak and stellarator plasmas. Below we summarize progress in several areas of MST research.

2. Confinement Performance

Improved confinement plasmas in MST are well established using current profile control to reduce MHD tearing instabilities, which can otherwise lead to large magnetic stochasticty [1,2]. Past optimization of the inductive current drive has concentrated on lower density conditions, likely related to maintaining high plasma conductivity in the outer region of the plasma. The density has now been increased to values substantially larger than the empirical (Greenwald) limit, using frozen pellet injection to concentrate the fueling in the core [3]. Edge-fueled RFP plasmas appear to obey the same density limit value observed in tokamak plasmas, i.e., $n_G \sim I_p / \pi a^2$ [4]. In pellet-fueled plasmas, a normalized density up to $n/n_G = 1.5$ has been obtained during the transient improved confinement period in 0.2 MA plasmas, and an MST record-high density $n = 0.7 \times 10^{20}$ m^{-3} ($n/n_G = 1.1$) is achieved at 0.5 MA (see Fig. 1). While improved relative to standard RFP plasmas, the reduction in magnetic fluctuations is less than obtained at lower density. Linear stability calculations indicate that pressure-driven tearing could be important, while the measured pressure profile can exceed the Mercier criterion in the core [3]. A hard (or disruptive) density limit has not been observed in MST.
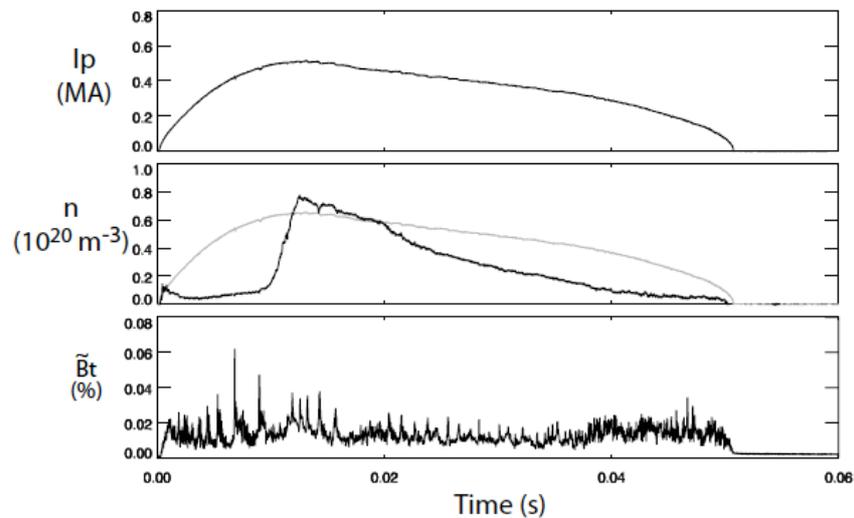

FIG. 1. High density MST plasma. Top panel is the plasma current, middle panel is the line-average density, with the Greenwald density shown in gray, and the bottom panel is the normalized r.m.s. magnetic fluctuation amplitude for m=1 modes. Frozen deuterium pellets were injected at 9 ms, just before inductive profile control programming was initiated at 12 ms.

Maximum energy confinement of $\tau_E = 12$ ms is obtained in MST at 0.5 MA and lower density, $n/n_G = 0.13$ [5]. This is a record value for the RFP. The electron temperature profile is peaked, with maximum on-axis $T_e(0) \approx 2$ keV for line-average density $n \approx 10^{19}$ m^{-3}. This τ_E is within a factor of two of expectations for a tokamak of the same size, current, and heating power, thus establishing tokamak-like confinement over MST's full range of plasma current. Fig. 2 shows the confinement measured in MST at low and high current for standard and improved confinement (PPCD) on the IPB98(y,2) ELMy-H mode empirical tokamak confinement scaling plot [6]. The MST data are plotted against the expected values for a same-size, same-current tokamak plasma, except the toroidal field is order ten-times smaller in MST. We emphasize this does not imply tokamak scaling applies to the RFP, rather simply provides a visual comparison of the confinement.
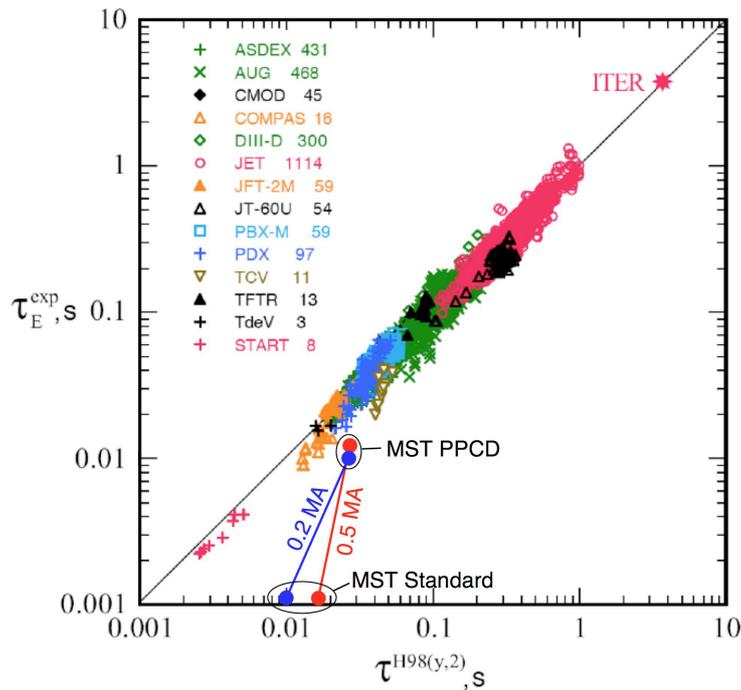

FIG. 2. Tokamak-like confinement in MST. The measured global energy confinement time for high and low current plasmas in MST are plotted at the expected values for a tokamak plasma of the same size, same current, and same heating power.

An alternate path to improved RFP confinement has emerged in recent years based on the concept of single-helicity magnetic self-organization [7]. Normally, a broad spectrum of $m=1$ and $m=0$ modes of similar size appear, causing the magnetic field to become globally stochastic. In the single helicity state, the dynamo self-organization process would occur with only one mode. Experimentally, quasi-single-helicity (QSH) conditions are observed where one mode grows to large amplitude, while the "secondary modes" remain small, ideally vanishing in amplitude so that global stochasticity is mitigated. In the RFX device, the QSH state is observed to be preferred as the plasma current is increased. Cases where the dominant mode causes the core to attain a helical equilibrium are called single-helical-axis (SHaX) states [8]. The QSH state is also observed in MST, with a similar tendency for preference at high current and low density [9]. An example is shown in Fig. 3, with a ratio of the dominant mode amplitude to r.m.s. secondary mode amplitude of at least 10, exceeding the threshold

for onset of SHaX as observed in RFX. The electron temperature measured by Thomson scattering is shown for the core region and edge region. Analysis of energy confinement in such plasmas is underway. The decrease in SXR emission after 30 ms indicates the temperature is decreasing in time. Even though the QSH spectral condition is maintained for the bulk of the shot, the secondary mode amplitudes slowly rise after attaining their minimum values around 30 ms. This plasma is locked, no doubt a consequence of the very large dominant $n=5$ mode. Broadband magnetic field errors appear to grow steadily in time, ending with a value indicated by the residual fluctuation amplitude when the plasma current terminates at about 60 ms. Energy confinement in MST strongly correlates with the amplitude of the broadband secondary modes [10].
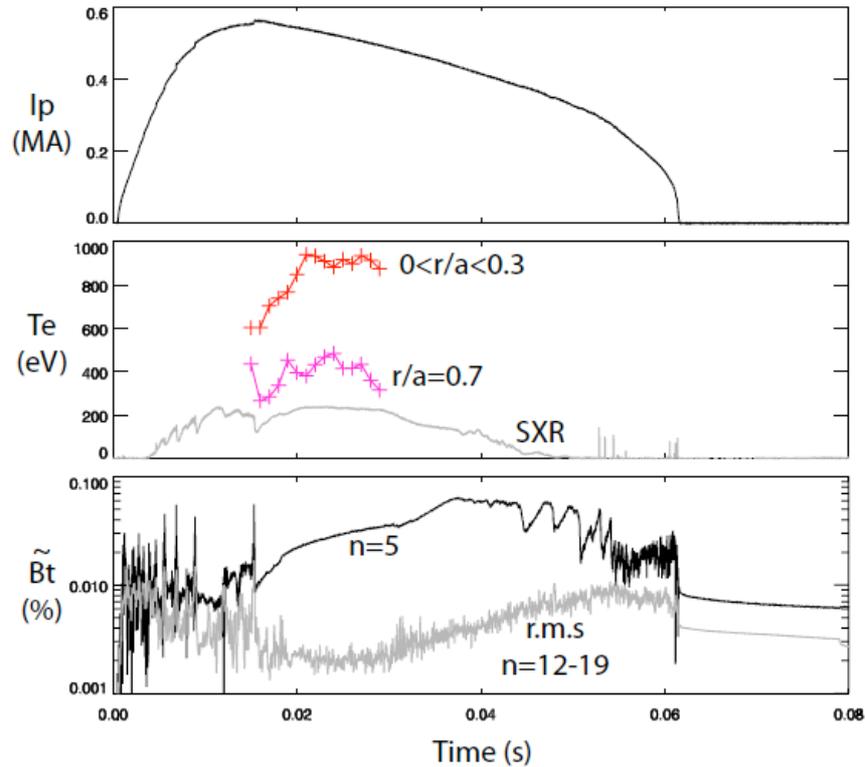

FIG. 3. Quasi-single-helicity plasma at high current in MST. Top panel is the plasma current, middle panel is the electron temperature measured by Thomson scattering at two radii, along with soft-x-ray emission, and the bottom panel are normalized amplitudes of m=1 magnetic fluctuations. The dominant mode (n=5) is ten-times larger than the r.m.s. amplitude of the secondary modes.

3. Neutral Beam Injection

A new 1 MW, 25 keV, tangential neutral beam injector (NBI) has been installed on MST. The extremely compact injector (shown in Fig. 4) produces a 20 ms NBI pulse to enable first-time investigations of several beam-plasma interactions in RFP plasmas. Modeling using TRANSP predicts a centrally peaked fast ion profile, with a fast ion pressure up to 50% of the thermal pressure. The confinement of the energetic ions is assessed using the decay of d-d fusion neutrons at NBI turn-off, as shown in Fig. 5. In this case the NBI is abbreviated to 5 ms, allowing analysis of the energetic ions in improved confinement plasmas (PPCD). Modeling is performed for the classical slowing down of the ions using the measured density,

temperature, and neutral particle content. The confinement time is a parameter determined by best fit to the d-d neutron rate, in this example at least 20 ms. This result confirms previous measurements with a very short pulse beam and smaller number of energetic ions [11].

The NBI injected ions are observed to impart a significant torque on the plasma. The tearing mode resonant closest to the magnetic axis is also affected. This is shown in Fig. 6. Moderate current plasmas with edge safety factor $q_a = 0$ are compared with and without NBI. TRANSP predicts that the fast ion profile should be centrally peaked. (Fast ion diagnostics are under construction.) It is therefore perhaps not surprising that the inner most $n=5$ mode is most affected, with its amplitude maintained smaller with NBI. The change in the profile of the toroidal rotation is indicated by the phase velocities of the $n=5-7$ modes, whose resonant surfaces span the core region out to $r/a \approx 0.5$. The increased mode rotation evidences the external torque being applied by NBI. The larger increase in the $n=5$ rotation relative to the other modes evidences the flow profile is more strongly sheared. A toroidally viewing line-average impurity ion Doppler spectrometer (IDS) measurement for fully-stripped carbon

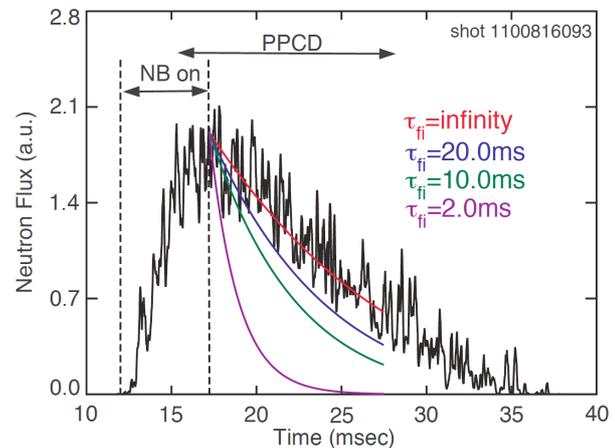FIG. 4. Compact neutral beam injector.

FIG. 5. The d-d neutron rate for NBI injection. An abbreviated 5 ms NBI pulse is applied from 12-17 ms, just before the application of inductive profile control (PPCD). The colored solid lines show the projected neutron decay rate for classical slowing down and varying fast ion confinement times.
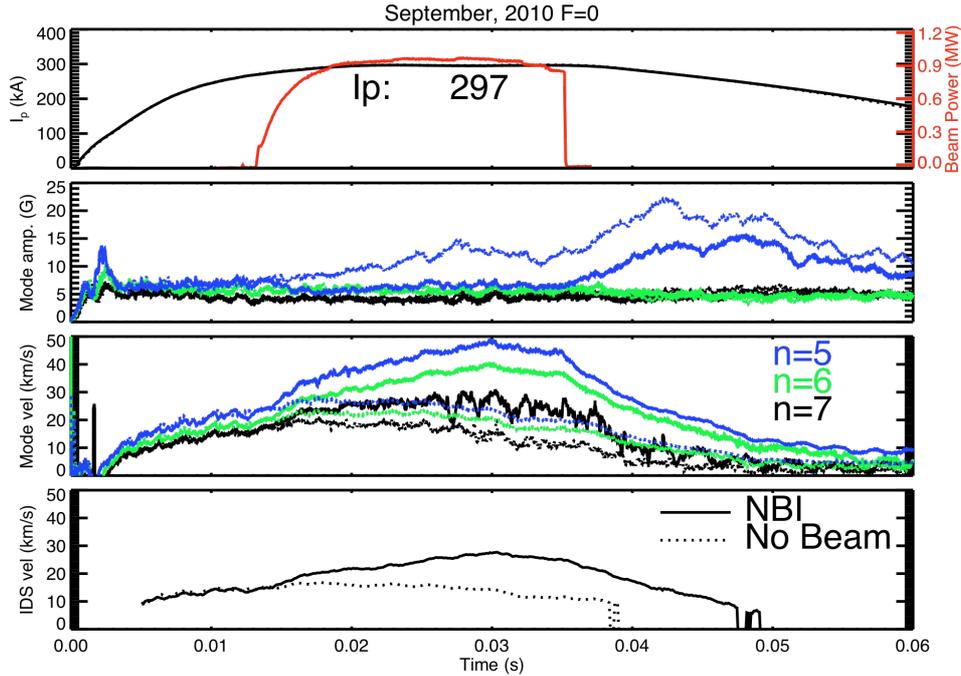
impurity ions correlates well with the $n=7$ mode phase velocity. This means the carbon profile likely peaks near mid-radius. Local measurements using CHERS are underway.

The 25 keV ions created by NBI are super-Alfvénic. It is therefore possible that the energetic ions could excite Alfvén eigenmodes, a topic that is barely studied in the RFP. Linear analysis has been performed for the RFP magnetic equilibrium by adapting codes developed for stellarator and tokamak research to determine the theoretical structure of TAE modes in the RFP. High frequency magnetic fluctuation measurements are underway to look for such modes. The high-bandwidth interferometer-polarimeter installed on MST will be extremely useful to study these modes, if they can be excited.

FIG. 6. External torque from NBI injection. Top panel shows the plasma current and NBI pulse, the second panel shows the amplitude of the n=5-7 tearing modes with (solid) and without (dashed) NBI, the third panel shows the toroidal phase velocity of the n=5-7 modes, and the fourth panel shows the chord-averaged impurity ion toroidal flow speed measured by Doppler spectroscopy. Increased flow-shear in the core region is evident in the relative changes of the mode phase velocities.

4. Current Drive and Heating

Steady-state current sustainment is extremely challenging for the RFP, given the small magnitude of the neoclassical bootstrap current. A potentially efficient and simple current drive method has been proposed that uses low frequency loop voltage oscillations to inject magnetic helicity. This is called oscillating field current drive (OFCD), and is being tested on MST. Previous work demonstrated that up to 10% of the plasma current can be sustained by the addition of OFCD (supplementing the background steady induction) [12]. This current increase is shown in Fig. 7, depending on the relative phase δ between the toroidal and poloidal loop voltage oscillations. The fraction of current drive (~10%) produced by these moderate-power OFCD experiments agrees well with nonlinear, 3D resistive MHD computation, reinforcing the OFCD physics basis [13]. This modeling also reproduces the measured dependence of the OFCD current drive on the relative phase δ between the ac loop voltages.

The energy confinement has now been measured during OFCD [14]. While the plasma pressure varies substantially during the ac cycle, as shown in Fig. 8, the cycle-average energy confinement is about the same as for standard steady induction for the case of maximum current drive. This is consistent with the cycle-average amplitudes of the tearing modes also about the same as for steady induction. (There is actually a modest reduction in the $m=0$ amplitude with OFCD.) This is a promising result, since the OFCD concept relies on a magnetic self-organization process, and attainment of at least as good confinement as for

steady-induction maintains the possibility for practical application in high current, high temperature plasmas. For relative oscillator phases where magnetic helicity is removed (anti-current drive), the magnetic fluctuations are increased, and the energy confinement is degraded.
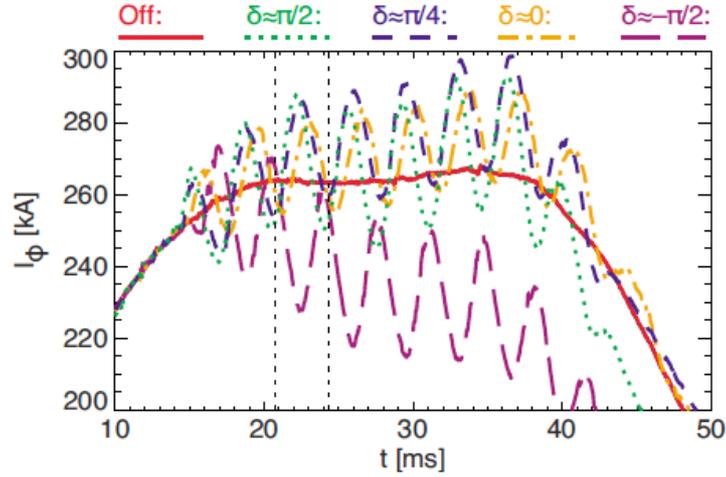

FIG. 7. *The plasma current for several OFCD cases where the relative phase between the toroidal and poloidal loop voltage oscillations is varied. Both current drive and anti-current drive are expected as the phase is varied. These are compared to the steady-induction case (OFF) without OFCD.*
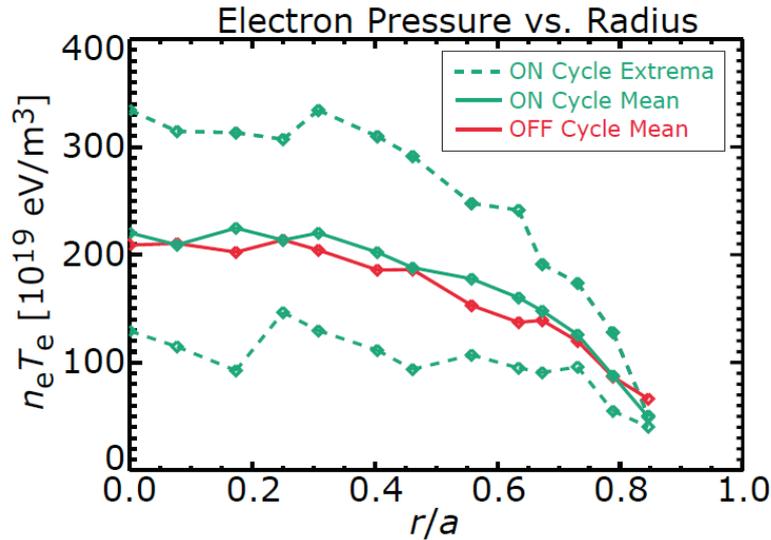

FIG. 8. *Profiles of the electron pressure for the $\delta=\pi/4$ case. The cycle-mean profile is indistinguishable from the OFCD off profile. The extremes of the pressure profile are show with broken lines.*

Lower-hybrid and electron Bernstein wave injection are in development for current drive and heating in MST. Modeling of the electric field in the antenna near-field, together with Monte Carlo test particle analysis, reproduces key features of the hard-x-ray emission observed with 125 kW coupled power of 800 MHz lower-hybrid waves. Soft-x-ray emission is observed for 100 kW injected power of 3.6 GHz waves into improved confinement target plasmas with

steep edge gradients suited for EBW mode conversion. A 1 MW, 5.5 GHz EBW experiment is in preparation.

5. Ion Heating, Fluctuations, and Transport

Powerful non-collisional ion heating is observed during magnetic reconnection events (sawteeth) in MST, with $T_i \approx 2 - 3$ keV in the largest events [5]. The energy reservoir for this heating is clearly the stored magnetic energy in the equilibrium magnetic field, but the process that transfers the energy to the ions is not fully understood. Generally it is believed that magnetic reconnection physics is involved. Several new measurements reveal features of the heating process that are expected to help identify the underlying physics. First, the fraction of equilibrium magnetic energy transferred to the ions is measured to increase with the majority ion mass, $\Delta T_i / \Delta W_{mag} \sim \sqrt{M_i}$ [15]. This is shown in Fig. 9. The Rutherford scattering of neutrals injected from a diagnostic neutral beam is used to infer the majority ion temperature in hydrogen, deuterium, and helium plasmas. The second new observation is that the heating is anisotropic, depending on the plasma density. This is shown in Fig. 10. In this case, the temperature of carbon impurity ions is measured using CHERS, localized to an interaction region defined by a second diagnostic neutral beam. Toroidal and poloidal views in the core region are used to determine the parallel and perpendicular ion temperature relative to the local field direction (toroidal in the plasma core). As the plasma density is increased, the anisotropy in the parallel and perpendicular temperatures is observed to increase. This behavior is observed globally throughout the plasma volume.
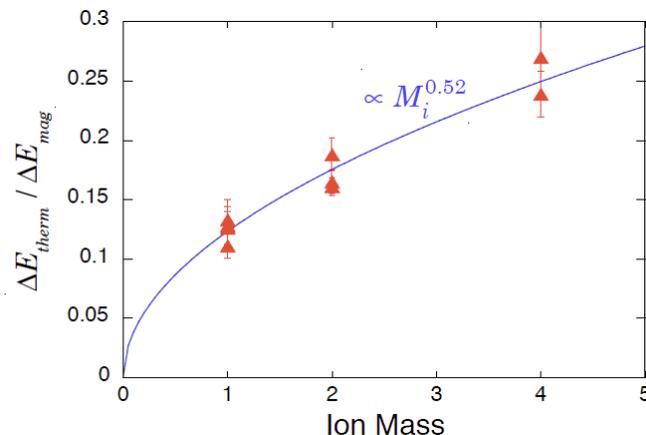

FIG. 9. The ion heating efficiency as a function of majority ion mass. The increase in ion thermal energy following a relaxation (sawtooth) event is normalized to the decrease in stored magnetic energy. This ratio increases with ion mass, indicating heavier ions are heated more efficiently.

A broad spectrum of magnetic turbulence has been measured with power-law features characteristic of a dissipative nonlinear cascade, perhaps connected to the ion heating mechanism [16]. Detailed probe measurements of the $m = 0$ reconnection layer reveal that the nonlinear Hall term in Ohm's law is a dominant driver for magnetic reconnection, reinforcing the importance of nonlinear mode coupling and two-fluid physics in magnetic self-organization dynamics.
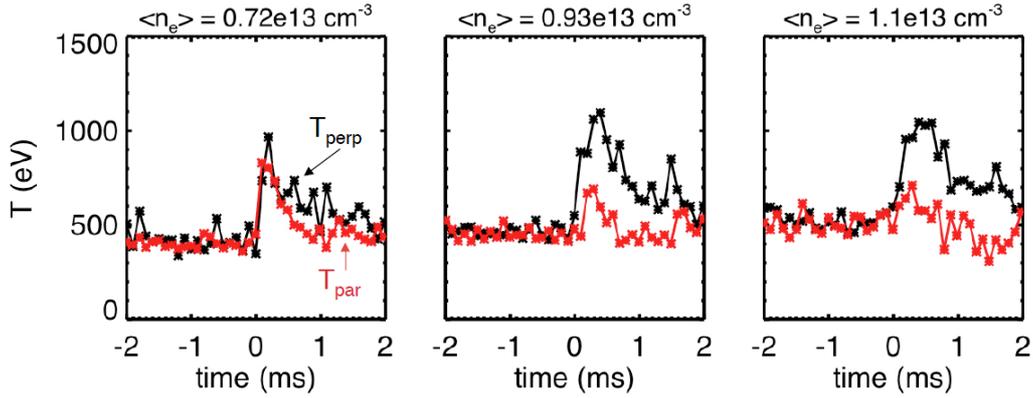
FIG. 10. The carbon impurity ion temperature during reconnection events in plasmas with varying density. All measurements are local using charge-exchange recombination spectroscopy (CHERS) and a diagnostic neutral beam. The parallel-perpendicular anisotropy increases with density.

Electron temperature fluctuations have been measured using a new high rep-rate Thomson scattering diagnostic that identifies flattening of the T_e profile in the vicinity of remnant magnetic island structures [17]. This is shown in Fig. 11. Temperature profile measurements are made at 22 radial locations, with a rep-rate of up to 25 kHz (30 pulses total for the present system) [18]. Correlating the temperature measurements with the toroidal modes measured at the plasma surface allows identifying the temperature fluctuation associated with a given toroidal mode, n. The typical mode rotation is order 10 kHz, so the fast Thomson measurements are able to resolve the rotating structures. Local peaking and a helical distortion of the T_e profile are seen for a mode resonant very near the magnetic axis.

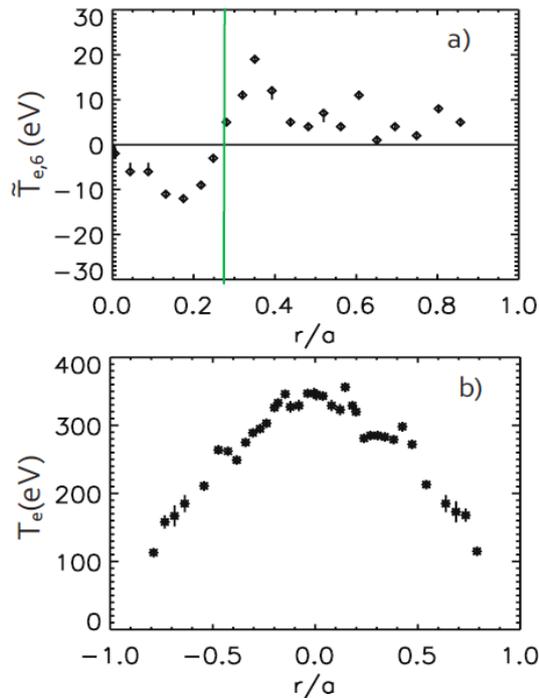*FIG. 11. (a) Electron temperature fluctuation amplitude associated with the m=1, n=6 tearing mode measured by Thomson scattering. (b) Calculated electron temperature across an X-point (left side) and O-point (right side) using measurements of the mean and fluctuating temperature components. The isothermal island is evident at the O-point.*

The mean and fluctuating electrostatic potential are being measured in the core of improved confinement plasmas using an improved heavy ion beam probe (HIBP) that is able to accommodate the rapidly changing magnetic equilibrium associated with inductive current profile control (PPCD), a great challenge for the HIBP diagnostic [19]. An example of the potential evolution is shown in Fig. 12. The HIBP also measures the fluctuations in the potential and density. This provides a great opportunity to investigate the role of electrostatic turbulence when the magnetic turbulence is greatly reduced. Previous analysis of energetic electrons indicates that electrostatic turbulent transport is possibly dominant in these improved confinement plasma conditions when magnetic turbulence is suppressed. New theoretical analysis using the GYRO code modified for RFP equilibria identifies that ion-temperature-gradient (ITG) instability is possible [20]. Relative to the well-studied tokamak case, the predicted mode structure is more extended along the field, and the critical temperature gradient is higher by order the aspect ratio, R/a. The linear growth rates as a function of the temperature gradient scale length are shown in Fig. 12. Note that the scale length is normalized to the minor radius.
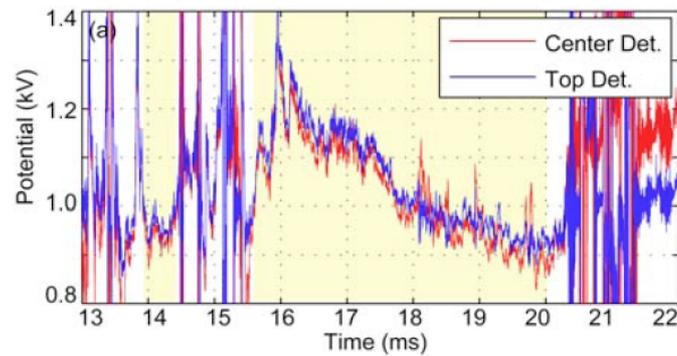

FIG. 11. Plasma potential measured by the HIBP in the core of improved confinement plasmas (PPCD). The gradual decrease in the potential likely corresponds to improved particle confinement.
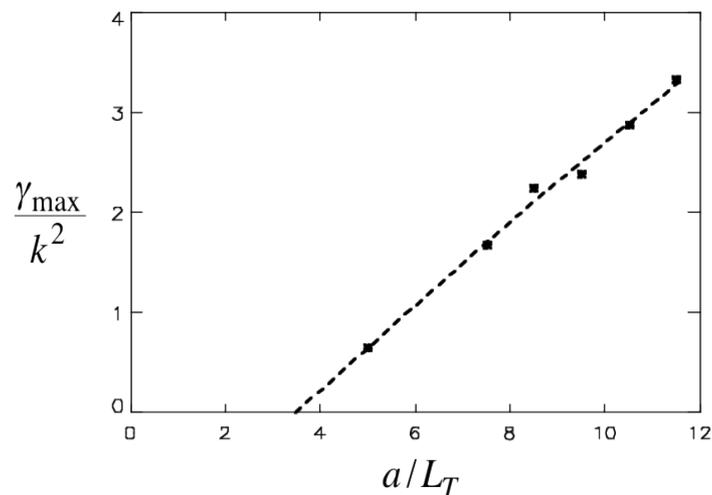

FIG. 12. Linear growth rates for ITG instability versus the normalized temperature scale length. These calculations were made using a modified version of GYRO capable of handling RFP equilibria.

[1] J.S. Sarff, J.K. Anderson, T.M. Biewer et al., Plasma Phys. Control. Fusion **45**, A457 (2003).

[2] B.E. Chapman, J.W. Ahn, A.F. Almagri et al., Nucl. Fusion **49**, 104020 (2009).

[3] M.D. Wyman, B.E. Chapman, J.W. Ahn et al, Nucl. Fusion **49**, 015003 (2009).

[4] M. Greenwald, "Density limits in toroidal plasmas," Plasma Phys. Control. Fusion **44**, R47 (2002).

[5] B.E. Chapman et al, "Generation and confinement of hot ions and electrons in a reversed field pinch plasma," to appear in Nucl. Fusion.

[6] ITER Physics Guidelines, ITER report N 19 FDR 1 01-07-13 R 0.1.

[7] D. Escande et al., Phys. Rev. Lett. **85**, 1662 (2000).

[8] R. Lorenzini et al. Nat. Phys. **5**, 570 (2009).

[9] P. Franz, L. Marrelli, P. Piovesan et al., Phys. Plasmas **13**, 012510 (2006).

[10] J.S. Sarff, A.F. Almagri, J.K. Anderson et al., Nucl. Fusion **43**, 1684 (2003).

[11] G. Fiksel, B. Hudson, D.J. Den Hartog et al., Phys. Rev. Letters **95**, 125001 (2005).

[12] K. J McCollam, A. P. Blair, S. C. Prager, J. S. Sarff, Phys. Rev. Lett. **96**, 035003 (2006).

[13] F. Ebrahimi, S.C. Prager, J.S. Sarff and J.C. Wright, Phys. Plasmas **10**, 999 (2003).

[14] K.J. McCollam, J.K. Anderson, A.P. Blair et al., Phys. Plasmas **17**, 082506 (2010).

[15] G. Fiksel, A.F. Almagri, B.E. Chapman et al, Phys. Rev. Lett. **103** 145002 (2009).

[16] Y. Ren et al., "Experimental observation of anisotropic magnetic turbulence in a reversed field pinch," submitted to Phys. Rev. Lett.

[17] H.D. Stephens, D.J. Den Hartog, C.C. Hegna, J.A. Reusch, Phys. Plasmas **17**, 056115 (2010).

[18] D.J. Den Hartog, "Pulse-burst laser systems for fast Thomson scattering," to appear in Rev. Sci. Instrum.

[19] D.R. Demers, X. Chen, P.M. Schoch, "HIBP Operation in Time Varying Equilibria of Improved Confinement RFP Discharges", to appear in Rev. Sci. Instrum.

[20] V. Tangri, P.W. Terry, R.E. Waltz, J.S. Sarff, "Gyrokinetic simulation of temperature gradient instability in the RFP," paper TH-C/P4-26 this conference.